Published OnlineFirst September 3, 2014; DOI: 10.1158/0008-5472.CAN-14-0471

apoptosis in paraffin-embedded sections using the In Situ Apoptosis Detection Kit as described by the manufacturer (Takara). Nuclei were stained with 4,6′-diamidino-2-phenylindole to count the total cells per crypt. A minimum of 10 crypts were counted per section.

Statistical analysis

Differences were analyzed using the Student *t* test. To compare variables of more than 2 conditions, ANOVO with *post hoc* Tukey–Kramer honestly significant difference (HSD) multiple comparison was applied. The relationship between the expression of several genes was analyzed by Spearman rank correlation test. $P < 0.05$ was considered significant.

Results

Correlation of Cirp expression with TNFα, IL23/IL17, Bcl-2, and stem cell marker expression in patients with IBD

Cirp expression correlated weakly but significantly with TNFα with a linear coefficient of 0.26 in the colonic mucosa of patients with ulcerative colitis (Supplementary Fig. S1A). In patients with Crohn disease, Cirp expression did not significantly correlate with TNFα (data not shown) probably because the majority of patients with Crohn disease enrolled in this study had undergone anti-TNFα therapy. IL23p19 is the specific subunit of IL23, a positive regulator of T_H17 and other IL17-producing cells (5). A significant correlation was found between *Cirp* and *IL17A* or *IL23p19* mRNA expression in patients with ulcerative colitis (Supplementary Fig. S1B and S1C) and in patients with Crohn disease (Supplementary Fig. S2A).

Defective apoptosis of inflammatory cell populations regulated by Bcl-2 seems to be a relevant pathogenetic mechanism in IBD (33, 34). There was a significant correlation between Cirp and Bcl-2 expression with a linear coefficient of 0.76 in patients with ulcerative colitis and with a linear coefficient of 0.60 in patients with Crohn disease (Fig. 1A and Supplementary Fig. S2B). Expression of Bcl-xL, another antiapoptotic protein, was significantly correlated with that of Cirp with a linear coefficient of 0.60 in patients with ulcerative colitis (Supplementary Fig. S1D) and with a linear coefficient of 0.85 in patients with Crohn disease (Supplementary Fig. S2C).

Stem cells, characterized by their ability to self-renew indefinitely and produce progeny capable of repopulating tissue-specific lineages, are critical for maintaining normal tissue homeostasis (35). Cirp is suggested to mediate the preservation of neural stem cells (18). Cirp expression correlated with Sox2, Bmi1, Lgr5, and Dclk1 levels with linear coefficients of 0.62, 0.45, 0.42, and 0.25, respectively, in patients with ulcerative colitis (Fig. 1B–D and Supplementary Fig. S1E) and correlated with Sox2 with a linear coefficient of 0.63 in patients with Crohn disease (Supplementary Fig. S2D). Cirp might be involved in regulation of intestinal inflammation and homeostasis maintenance in patients with IBD.

Increased Cirp expression in the colonic mucosa of patients with refractory ulcerative colitis

We next explored whether an association exists between Cirp expression and the clinical status of patients with ulcerative colitis. Refractory and nonrefractory active ulcerative colitis could not be distinguished by endoscopic findings (Fig. 2A). Cirp expression levels were specifically increased in patients with refractory ulcerative colitis associated with long-term inflammation, whereas similar expression levels of Cirp were found between normal colonic mucosa and the mucosa of patients with nonrefractory active ulcerative colitis (Fig. 2B). Similarly, increased Sox2 expression levels were found in the colonic mucosa of patients with refractory IBD (Fig. 2C). Immunohistochemistry showed that Sox2 was expressed in the mesenchyme and Dclk1 was expressed in the crypt of patients with refractory ulcerative colitis (Supplementary Fig. S3A and S3D). In contrast, increased TNFα expression was found in the colonic mucosa of both refractory and nonrefractory active ulcerative colitis (Fig. 2D). Immunohistochemistry was performed to identify the cells expressing Cirp in the human intestine, and inflammatory cells were found to express more Cirp protein than epithelial cells, whose expression pattern was similar in controls and patients with ulcerative colitis. In chronically inflamed mucosa, Cirp expression was enhanced in inflammatory cells (Fig. 2E and Supplementary Fig. S3B). Inflammatory cells preferentially but not exclusively expressed Cirp protein also in human CAC cases (Supplementary Fig. S3C).

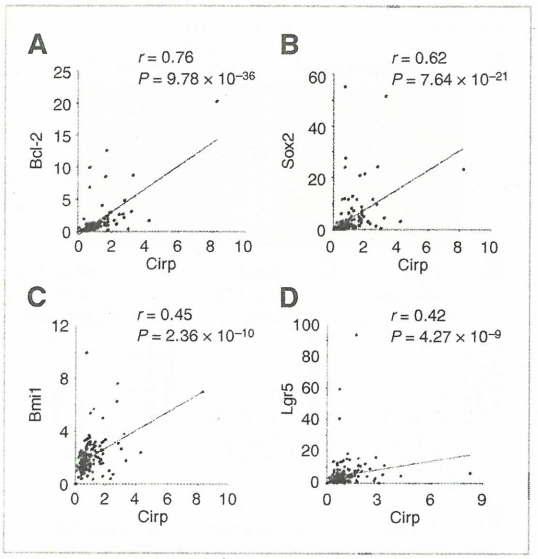

Figure 1. Association between Cirp and the expression of Bcl-2 and various stem cell markers in the colonic mucosa of patients with ulcerative colitis. Scatter plot of relative mRNA levels of Cirp and the respective genes (A, Bcl-2; B, Sox2; C, Bmi1; D, Lgr5) in human colonic mucosa.

Cirp$^{-/-}$ mice challenged with DSS have decreased susceptibility to inflammation

DSS-induced colitis is a murine model resembling human ulcerative colitis. Experimental colitis was induced by treating mice with 2.5% DSS. Histologic analysis revealed substantially less epithelial damage and disruption of crypt architecture in

Published OnlineFirst September 3, 2014; DOI: 10.1158/0008-5472.CAN-14-0471

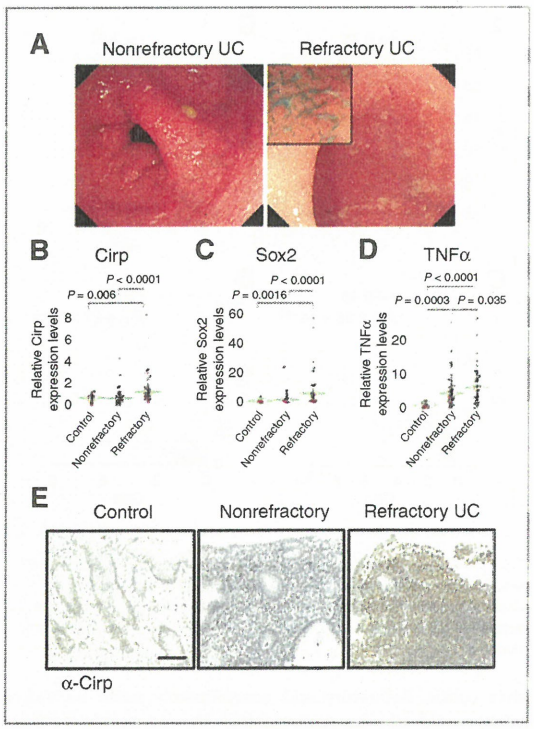

Figure 2. Cirp expression is increased in the colonic mucosa of patients with refractory ulcerative colitis (UC). A, endoscopic images of refractory and nonrefractory active ulcerative colitis specimens with a magnified inset. B–D, expression of Cirp (B), Sox2 (C), and TNFα (D) mRNA in normal colonic mucosa (control, $n = 30$), colonic mucosa of patients with nonrefractory active ulcerative colitis (nonrefractory, $n = 98$), and those with refractory ulcerative colitis (refractory, $n = 67$), as determined by quantitative real-time qPCR. *P* values were calculated by *post hoc* Tukey–Kramer HSD multiple comparison. The *F* and *P* values for the ANOVO test are as follows: $F(2, 192) = 11.98$; $P < 0.0001$ (B), $F(2, 192) = 10.29$; $P < 0.0001$ (C), and $F(2, 192) = 13.70$; $P < 0.0001$ (D). E, representative images of immunohistochemical findings in human colonic mucosa of patients without ulcerative colitis and those with nonrefractory and refractory ulcerative colitis. Scale bar, 50 μm.

Cirp$^{-/-}$ mice than in WT mice (Fig. 3A), and inflammatory cell infiltration into the colon was less in *Cirp*$^{-/-}$ mice (Fig. 3B). Immunohistochemically assessed macrophage infiltration was smaller in *Cirp*$^{-/-}$ than in WT mice after DSS administration (Fig. 3C), and the epithelial injury score was significantly smaller in the *Cirp*$^{-/-}$ mice than in the controls (Fig. 3D). Next, we compared apoptosis induction in DSS-treated WT and *Cirp*$^{-/-}$ mice. Apoptosis detected by TUNEL staining was observed in DSS-treated mice, primarily in the colonic crypts (Fig. 3E), but was blocked by 50% in the *Cirp*$^{-/-}$ mice (Fig. 3F). Examination of the colonic lysates from DSS-treated WT and *Cirp*$^{-/-}$ mice showed that the Cirp presence increased PCNA expression in the colon (Supplementary Fig. S4A).

The associated immune response was investigated by analyzing colonic cytokine levels. Colonic tissue from *Cirp*$^{-/-}$ mice showed a smaller immune response with lower levels of proinflammatory cytokine TNFα and IL23 than that of WT mice (Fig. 4A–C), which is consistent with the data in humans (Fig. 1 and Supplementary Fig. S1). TNFα expression was upregulated in nonrefractory active ulcerative colitis whereas Cirp expression was not in these patients (Fig. 2B and D). This is probably because TNFα is induced in both a Cirp-dependent and -independent manners in the colon. There was no significant difference in IL1β, IL10, and IL21 (Fig. 4B and Supplementary Fig. S4B). To explore the mechanisms of the effects of Cirp on TNFα production, we sought to confirm these findings *in vitro*. In lamina propria cells isolated from DSS-treated colons of Cirp-deficient mice, expression of TNFα and IL23 was decreased compared with those of WT mice (Fig. 4D). TNFα is produced chiefly by activated macrophages, although it can be produced by many other cell types as lymphocytes and natural killer cells (36), so we next isolated macrophages from DSS-treated colons. TNFα mRNA expression was significantly reduced in Cirp-deficient macrophages (Fig. 4E). Macrophages

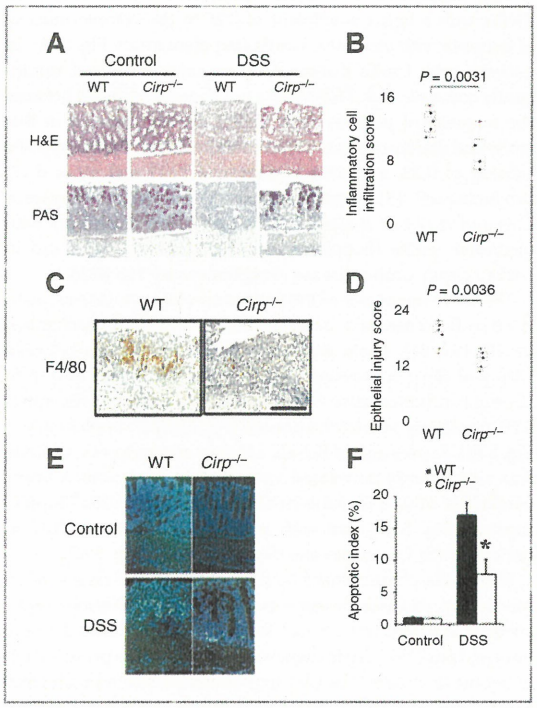

Figure 3. Susceptibility to inflammation is decreased in *Cirp*$^{-/-}$ mice challenged with DSS. A, representative photographs of H&E-stained and periodic acid—Schiff (PAS)-stained colons of WT and *Cirp*$^{-/-}$ mice 7 days after the initiation of DSS administration (original magnification, ×200). Scale bar, 50 μm. B, inflammatory cell infiltration into colonic tissues of WT and *Cirp*$^{-/-}$ mice 7 days after the initiation of DSS administration. Scoring was performed as described in Materials and Methods. $n = 6$ per group. C, representative images of immunohistochemical detection of F4/80, a marker for macrophages, in colonic tissue. Scale bar, 100 μm. D, histologic scoring of epithelial injury in colons. $n = 6$ per group. E, TUNEL staining of colonic tissues from DSS-treated mice (original magnification, ×200). F, the apoptotic index was measured by counting TUNEL signals in 100 randomly selected crypts. Results are expressed as means ± SEM ($n = 4$ per group). *, $P < 0.05$ compared with WT mice.

Published OnlineFirst September 3, 2014; DOI: 10.1158/0008-5472.CAN-14-0471

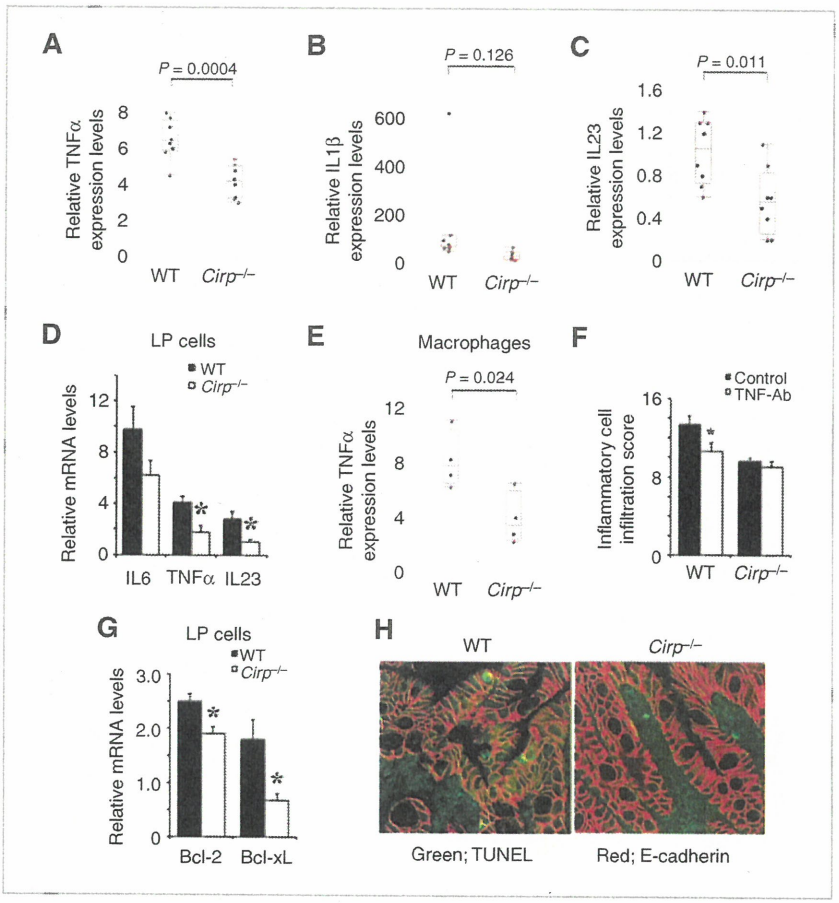

Figure 4. Cirp contributes to TNFα and IL23 production and Bcl-2 and Bcl-xL expression in inflammatory cells. A–C, relative levels of TNFα (A), IL1β (B), and IL23 (C) in colonic tissues from mice treated with DSS, as determined by real-time qPCR ($n = 8$ per group). Expression level in colonic tissues from nontreated WT mice was set as 1. D and E, effect of Cirp on gene expression in colonic lamina propria (LP) cells (D) and macrophages (E). Lamina propria cells and macrophages were isolated, and cytokine mRNA expression was analyzed by real-time qPCR. The mRNA expression levels in lamina propria cells or macrophages from nontreated WT mice were set as 1, respectively. Results are expressed as means ± SEM ($n = 4$ per group). *, $P < 0.05$ compared with WT mice. F, inflammatory cell infiltration into colonic tissues of WT and *Cirp*$^{-/-}$ mice 7 days after the initiation of DSS administration with or without anti-TNFα antibody treatment. Scoring was performed as described in Materials and Methods. $n = 3$ per group. *, $P < 0.05$ compared with control. G, effect of Cirp on gene expression in colonic lamina propria cells. Lamina propria cells were isolated, and cytokine mRNA expression was analyzed by real-time qPCR. The mRNA expression levels in lamina propria cells from nontreated WT mice were set as 1. *, $P < 0.05$ compared with WT LP cells. H, representative images of immunohistochemical detection of E-cadherin, a marker for epithelial cells, and TUNEL staining of colonic tissues from DSS-treated mice.

derived from WT bone marrow exhibited marked upregulation of TNFα mRNA relative to those derived from *Cirp*$^{-/-}$ bone marrow (Supplementary Fig. S4C). Cirp has been reported to activate NF-κB (25, 27). Consistently, the presence of Cirp increased IκBα phosphorylation in bone marrow–derived macrophages (Supplementary Fig. S4D). Treatment with anti-TNFα antibody reduced inflammatory cell infiltration in WT mice but not in *Cirp*$^{-/-}$ mice (Fig. 4F). These data indicate that Cirp in inflammatory cells augments the inflammatory response by producing cytokines such as TNFα and IL23. In addition, *Bcl-2* and *Bcl-xL* mRNA expression was significantly reduced in Cirp-deficient inflammatory cells (Fig. 4G), and more apoptosis was found in *Cirp*$^{-/-}$ immune cells than WT immune cells (Fig. 4H), which might at least partially contribute to the attenuated inflammatory responses by Cirp deficiency.

Cirp deficiency attenuated tumorigenesis in the murine CAC model

Chronic inflammation increases intestinal cancer risk in IBD (10). To investigate the precise pathogenic mechanisms underlying IBD-associated colorectal carcinogenesis, we used the AOM plus DSS mouse model to study the role of Cirp in CAC. In the AOM/DSS protocol, a significant decrease was noted in the number and maximum size of tumors in the *Cirp*$^{-/-}$ mice compared with WT mice (Fig. 5A and B). Histologic

Published OnlineFirst September 3, 2014; DOI: 10.1158/0008-5472.CAN-14-0471

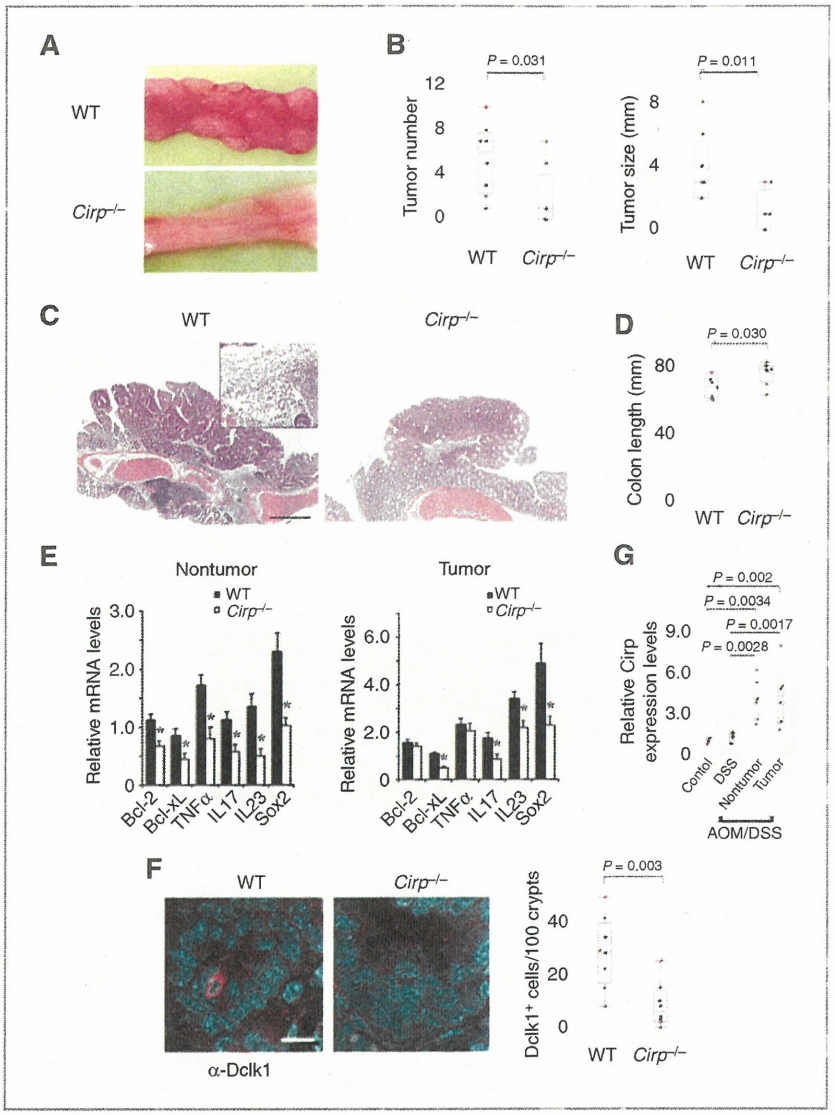

Figure 5. Cirp deficiency affects colonic tumorigenesis in a murine model of CAC. A, typical examples of macroscopic tumorigenesis in the CAC model. Colons were cut longitudinally. B, tumor number and maximum size (WT mice, $n = 8$; $Cirp^{-/-}$ mice, $n = 8$). C, typical examples of microscopic tumorigenesis in the CAC model with magnified insets. Scale bar, 500 μm. D, colon length after treatment with AOM and DSS. E, RNA was extracted from nontumorous colon and tumor tissues. Relative amounts of mRNA, as determined by real-time qPCR normalized to the amount of actin mRNA. The amount of each mRNA in the untreated colon was given an arbitrary value of 1.0. *, $P < 0.05$ compared with WT mice. F, immunohistochemical findings of colon sections of AOM/DSS-treated WT and $Cirp^{-/-}$ mice. The tumor bases stained with anti-Dclk1 antibody were identified by confocal microscopy. Scale bar, 15 μm. G, RNA was extracted from the colonic tissues of WT mice 7 days after the initiation of DSS administration (DSS, $n = 8$) and nontumorous colon and tumor tissues of WT mice after administration of AOM and DSS (DSS + AOM, $n = 6$). Relative amounts of mRNA as determined by real-time qPCR and normalized to the amount of actin mRNA. The mean value of mRNA in untreated colon (control, $n = 5$) was given an arbitrary value of 1.0. *P* values were calculated by *post hoc* Tukey–Kramer HSD multiple comparison.

examination of H&E-stained sections from the rolled-up colons revealed larger adenomas with a complex tumor growth pattern in WT tumors compared with $Cirp^{-/-}$ tumors (Fig. 5C). Extensive infiltration of inflammatory cells into the lamina propria and submucosal layer surrounding the tumors suggest the involvement of inflammatory responses in the tumorigenesis seen in the AOM/DSS-treated mice (Fig. 5C). Colon length was measured as one parameter to assess the severity of inflammation and was found to be significantly longer in $Cirp^{-/-}$ mice than in WT mice (Fig. 5D). The expression of TNFα was decreased in nontumorous tissue, but not in tumors, of $Cirp^{-/-}$ mice challenged with AOM and DSS (Fig. 5E). Tumor and nontumor cells would use different mechanisms to regulate gene expression. In tumor cells, expression of TNFα might be upregulated in a Cirp-independent manner. IL23 and IL17 inhibit antitumor immunity and promote tumorigenesis (6–8). Expression of IL23 and IL17 was decreased in $Cirp^{-/-}$ tumors and nontumor colons compared with WT counterparts (Fig. 5E). *Bcl-2* and *Bcl-xL* mRNA expression that is upregulated by Cirp in inflammatory cells (Fig. 4G) was significantly reduced in Cirp-deficient colons (Fig. 5E). Cirp deficiency decreased proliferating cell nuclear antigen (PCNA) expression in DSS-treated colons, whereas in established tumors, neither apoptosis nor PCNA expression was significantly affected by Cirp deletion (Supplementary Fig. S6). The expression of stemness factor Sox2 was decreased in Cirp-deficient colons

Published OnlineFirst September 3, 2014; DOI: 10.1158/0008-5472.CAN-14-0471

and tumors compared with WT tissues (Fig. 5E and Supplementary Fig. S5A). Dclk1 is a candidate tumor stem cell marker in the gut (37). Deletion of Cirp decreased the number of Dclk1$^+$ cells at the tumor base (Fig. 5F).

Cirp expression was increased in the colonic mucosa of tumor-harboring mice given DSS and AOM, whereas short-term inflammation induced by DSS administration for 7 days did not upregulate Cirp expression (Fig. 5G and Supplementary Fig. S5B). Coupled with the findings in humans (Fig. 2B and E), these results suggest that Cirp is induced by long-term intestinal inflammation.

Cirp promotes tumorigenesis through hematopoietic cell populations

To functionally characterize the contribution of different cell populations to colorectal tumorigenesis, we created Cirp chimeric mice using a combination of γ-irradiation and BMT. Nontransplanted controls survived less than 2 weeks after irradiation, indicating there was ablation of the endogenous marrow. Transplanted animals were allowed to recover for 2 months before placing them on the AOM/DSS protocol. WT mice rescued with *Cirp*$^{-/-}$ bone marrow had a significantly smaller tumor burden than those rescued with WT bone marrow (Fig. 6A and B). Both WT and *Cirp*$^{-/-}$ mice rescued with WT bone marrow had equivalent tumor sizes (Fig. 6B). Chimeras harboring *Cirp*$^{-/-}$ bone marrow diminished expression of TNFα (Fig. 6C), which indicates that Cirp in hematopoietic cells is involved in upregulation of TNFα. Cirp-chimeric mice with Cirp-deficient bone marrow showed a smaller number of Dclk1$^+$ and Sox2$^+$ cells in tumor than in the WT mice (Fig. 6D and E). Taken together, at least in this model, the absence of Cirp in hematopoietic cellular compartments protects against AOM/DSS-induced tumorigenesis.

Discussion

The association between IBD and colorectal cancer is well established; the cumulative risk of developing colorectal cancer after 20 years is 7% in ulcerative colitis and 8% in Crohn disease (10). Optimal IBD management would reduce the risk of CAC (35). While it is clear that chronic mucosal inflammation plays a causative role in the transition to adenocarcinoma, the molecular link between inflammation and cancer remains to be elucidated. AOM is a procarcinogen that is metabolically activated to a potent alkylating agent that forms O^6-methylguanine (38). Its oncogenic potential is markedly augmented in the setting of chronic inflammation, such as that induced by repeated cycles of DSS treatment (39). TNFα, a key mediator of inflammation in IBD (3), contributes to tumorigenesis by creating a tumor-supportive inflammatory microenvironment

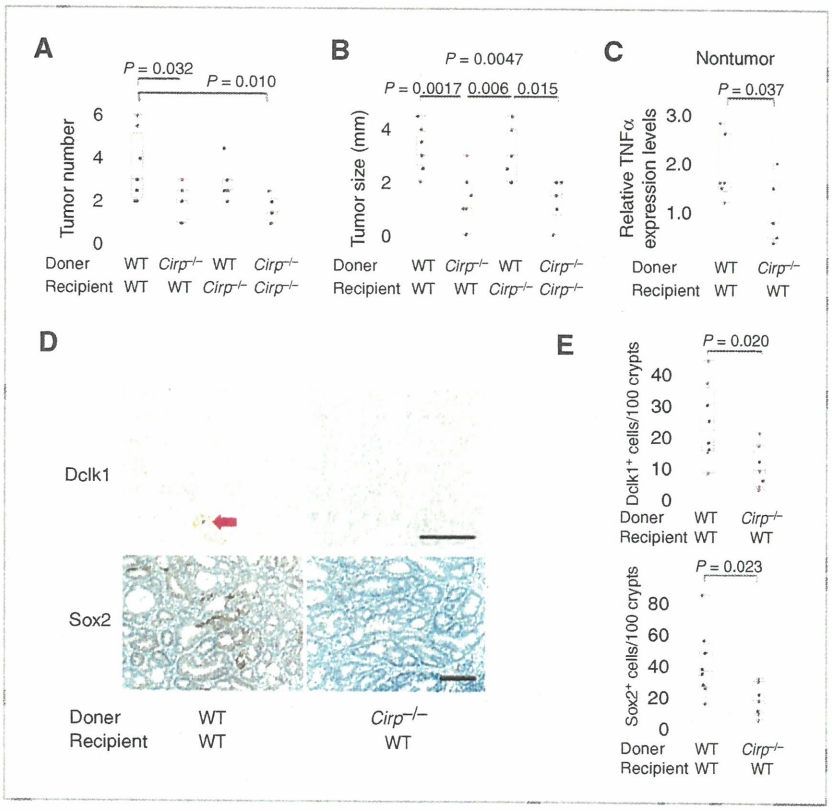

Figure 6. Cirp promotes tumorigenesis through hematopoietic cell populations. WT mice with WT or *Cirp*$^{-/-}$ bone marrow (BM) and *Cirp*$^{-/-}$ mice with WT or *Cirp*$^{-/-}$ bone marrow were generated by BMT. Number (A) and maximum size (B) of the tumors (WT-BM/WT mice, $n = 8$; *Cirp*$^{-/-}$-BM/WT mice, $n = 7$; WT-BM/*Cirp*$^{-/-}$ mice, $n = 7$; *Cirp*$^{-/-}$-BM/*Cirp*$^{-/-}$ mice, $n = 6$). *P* values were calculated by *post hoc* Tukey–Kramer HSD multiple comparison. C, RNA was extracted from nontumorous colon. Relative amounts of mRNA as determined by real-time qPCR normalized to the amount of actin mRNA. The amount of TNFα mRNA in the untreated colon was given an arbitrary value of 1.0. $n = 6$ per group. D, representative images of immunohistochemical detection of Dclk1 at the tumor base and Sox2 in tumors. Scale bar, 100 μm. E, the number of Dclk1$^+$ cells at the tumor base and Sox2$^+$ in tumors.